

**POTENTIAL USE OF GROUND-BASED LONG-WAVELENGTH RADAR FOR INTERIOR SENSING OF APOPHIS IN 2029.** M. S. Haynes<sup>1</sup>, C. Elachi<sup>2</sup>, L.A.M. Benner<sup>1</sup>, G. Hallinan<sup>2</sup>, I. Fenni<sup>1</sup>, B. Davidsson<sup>1</sup>, M. Brozovic<sup>1</sup>, P. Bernhardt<sup>3</sup>, J. Matthews<sup>3</sup>, J. Lazio<sup>1</sup>. <sup>1</sup>Jet Propulsion Laboratory, California Institute of Technology (4800 Oak Grove Dr. M/S 300-235, Pasadena, CA. [mark.s.haynes@jpl.nasa.gov](mailto:mark.s.haynes@jpl.nasa.gov)), <sup>2</sup>California Institute of Technology, Pasadena, CA. <sup>3</sup>University of Alaska - HAARP, Fair Banks, AK.

### Introduction:

Radar observations at frequencies of 100 MHz and lower have a long history of being used to probe the substructures and interiors of planetary bodies, with notable examples including the Apollo sounders at the Moon, MRO/MARSIS at Mars, and the Rosetta/CONSERT experiment at 67P. The 2029 close approach of Apophis offers an unprecedented opportunity to probe the interior of a Near Earth Asteroid using ground-based long-wavelength radar/radio [1]. Investigating ground-based long-wavelength (HF/VHF/UHF, 10-500 MHz) radar for this purpose is relatively new [2,3,4]. An initial list of potential observatories was reported in [1] and expanded in [4], with a subset given in Table 1 and Figure 2. We report results on the potential of using these facilities to observe Apophis in 2029. We expect long wavelengths to be sensitive to the interior with the ultimate goal of limited tomographic imaging of the internal structure.

**Background:** Knowledge of asteroid interiors is crucial for planetary defense but few methods exist for this purpose. The scientific goals of long-wavelength radar are to constrain the internal structure and composition (via the dielectric constant) and assess the internal material distribution (heterogeneity, presence of monoliths, size distribution of boulders) [2,5,6]. Porosity or other characteristics of the interior affect possible deflection and mitigation strategies. Radar products needed to meet these science goals are any of: 1) transmission time-of-flight (like Rosetta/CONSERT [7]), 2) volumetric backscatter from 3D synthetic aperture radar, or 3) 3D images of the dielectric constant formed using inverse scattering methods [8]. For ground-based systems both monostatic backscatter and limited-angle bistatic observations are possible.

Long radar wavelengths are required to penetrate the interior to overcome both scattering and absorption loss. We expect <0.5 dB/meter of absorption for frequencies <100MHz (see Table 1). Assuming 10 wavelengths of penetration, the lowest frequencies (e.g., 9.5 MHz) may cover most of the interior. Interior imaging also requires

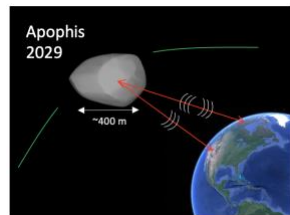


Figure 1: Cartoon of Apophis 2029 encounter and ground-based radar observation. Not to scale.

good SNR, long coherent integration times, and ionospheric compensation at frequencies <100 MHz, and 3D tomographic SAR is only possible with multiple viewing angles.

**Long-Wavelength Observatory Coverage During Apophis Encounter:** Figure 3 shows the local elevation angle of Apophis versus time from closest as viewed from the observatories listed in Table 1. The data were extracted from the JPL Horizons online ephemeris system. The lowest pointing capability depends on observatory. For example, despite high observation angles, the Jicamarca array (not listed) cannot actively steer to follow the asteroid. For most observatories in North America, Apophis will have a high elevation near closest approach and will not set for EISCAT-Svalbard in the second half of the encounter.

Observatory	Frequency (MHz)	Wavelength (m)	Estimated Attenuation (dB/m)	Apophis Max Elv. Angle (°)
HAARP	9.5	32	0.027	62
OVRO-LWA	12-85	25-3.5	0.035-0.24	88
CMOR	17, 30, 38	18, 10, 8	0.05 – 0.11	83
MU Radar	47	6.4	0.14	82
EISCAT 3D	233	1.3	0.67	41
EISCAT, Sv.	500	0.6	1.4	32
ALTAIR	158, 430	1.9, 0.7	0.45 – 1.2	78
LOFAR	10-240	30-1.3	0.029 – 0.7	58
MISA	440	0.68	1.3	82

Table 1: Long-wavelength radar/radio observatories. Attenuation in S-type asteroids estimated from [5] ( $\epsilon_r = 10$ ,  $\tan\delta = 0.01$ ). Maximum elevations angles taken from Figure 2.



Figure 2: Geographical location of long-wavelength radar/radio observatories in Table 1.

**Body-fixed Look Directions During Encounter for Radar Tomography:** The quality of backscatter 3D tomographic SAR depends on the number and angular diversity of radar viewing angles in the body-fixed

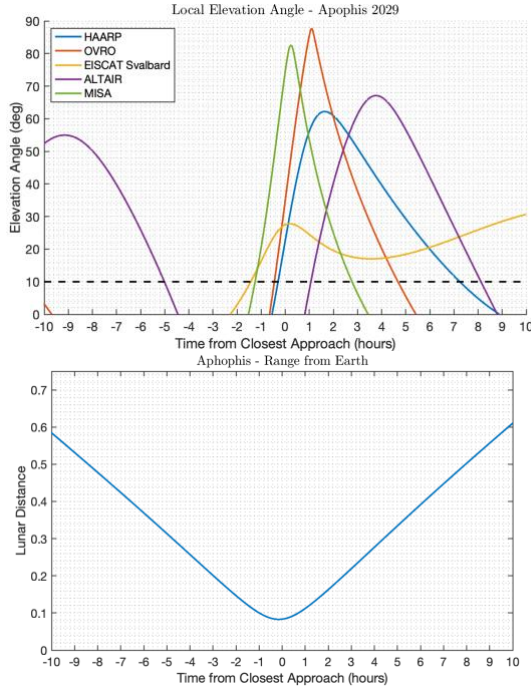


Figure 3: Top: Local elevation angles of Apophis during the encounter as viewed from select observatories in Table 1 (dashed line is 10° cutoff). Bottom: Apophis Range to Earth.

frame, [9]. We assess the evolution of viewing angles due to body rotation, Earth rotation, and sky motion, which will cover ~170 deg in 12 h around the epoch of closest approach. The estimated rotation period is 30.6 [10], however, the angular momentum vector cannot be meaningfully predicted in 2029 this far in advance.

Although Apophis tumbles slowly and tidal forces are expected to change the spin state during the encounter, we assume a principal axis rotator with constant spin axis defined as the ecliptic normal and spin phase referenced to closest approach. Figure 4 shows the body-fixed look angle to Earth during the encounter showing the potential for HAARP to view almost a full rotation.

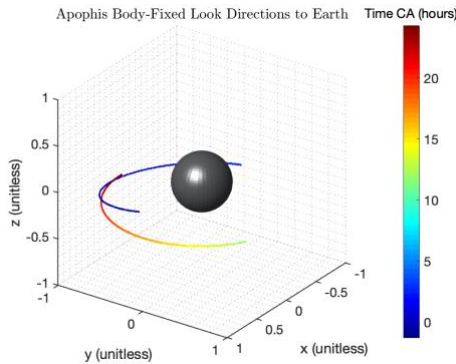


Figure 4: Body-fixed look directions to Earth from Apophis vs time from closest approach for HAARP for the first two observing windows and elevation angle >10°. Sky motion and rotation allow views of a large part of the surface.

**SNR at 7 MHz using HAARP and 60 MHz using**

**OVRO:** The principal limitation of long wavelength radar is less antenna gain for the same sized dish antennas compared to higher frequencies, therefore facilities with high-transmit power or distributed receiver arrays are desirable. The HAARP transmitter in Alaska operates from 2-10 MHz and is capable of ~3.6 GW EIRP. The estimated return power at 6.8 MHz is -149 dBmW at 100,000km, which is detectable by the AERE array adjacent to HAARP. The estimated backscatter SNR of the OVRO-Long Wavelength Array and OVRO 40-m dish transmitting a hypothetical 10 kW of power at 60 MHz is >20 dB. This shows that sensing Apophis with these facilities is possible.

**Backscatter Simulation of a Rubble Pile at 9.5**

**MHz:** Full-wave modeling of 3D rubble pile models is necessary to assess the sensitivity of interior imaging. The electrical size of Apophis is ~12λ at 9.5 MHz which can be simulated with today’s electromagnetic solvers. Figure 5 shows a rubble pile model of ~5e5 spheres with random dielectric constants bounded by a shape estimate of Apophis, [10], and monostatic backscatter at 9.5 MHz that will be used in future link budgets.

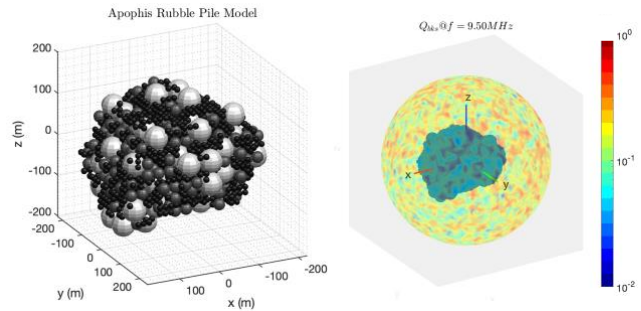


Figure 5: Left: Apophis rubble pile model. Right: simulated backscatter efficiency over the sphere of backscatter directions at 9.5 MHz.

**Future work:** We hope to conduct tests before 2029 notably on asteroids 2001 WN<sub>5</sub>, a 900-m-sized object that will approach within 0.7 lunar distances in June, 2028 and possibly 2010 XC15 in late 2022.

**Acknowledgments:** Part of this research was carried out at the Jet Propulsion Laboratory, California Institute of Technology, under a contract with NASA (80NM0018D0004). © 2022. All rights reserved.

**References:** [1] Nolan, M., et al (2020) *Apophis T-9*, 2242. [2] Herique, A., et al. (2020) *AT-9*, 2029. [3] Virkki, A., et al. (2020) *AT-9*, 2013. [4] Haynes, M., et al. (2022) *LPSC 1297*. [5] Herique, A., et al (2018) *Adv. Sp. Rch.*, 62, 2141-2162. [6] Haynes, M., et al., (2020) *NASEM PSDS*. [7] Kofman, W., et al. (2007) *Sp. Sci. Rv.* 128(1-4), 413-432. [8] Haynes, M., et al. (2021) *LPSC 2548* [9] Haynes, M., et al. (2021) *Adv. Sp. Rch.* 68, 3903-3924. [10] Brozovic, M., et al. (2018) *Icarus* 300, 115-128.